Drought by Design? How Rainfall Data Choices Shape Food Insecurity Estimates

Musa Hasen Ahmed*[1]

[1]Independent Researcher, Ethiopia

3rd November 2025

Abstract

This study combines household survey data from Mali and Chad with ten rainfall datasets from various sources to examine how the choice of rainfall data influences estimates of drought impacts on food security. Rainfall shocks are measured using the Standardized Precipitation Index and assigned through bilinear, nearest-neighbor, and zonal aggregation techniques. Results without controls reveal substantial heterogeneity. Estimated coefficients vary widely in both magnitude and sign across datasets and interpolation methods, with coarse or satellite-only products exhibiting particularly high volatility. Once controls are added, this heterogeneity largely disappears and coefficients converge toward consistently negative values in line with theoretical expectations. Beyond magnitudes, the analysis also finds that the relative ranking of datasets shifts depending on the interpolation method and model specification, revealing instability in dataset performance. The findings highlight a fundamental challenge for applied economics since empirical conclusions may depend as much on dataset choice, spatial interpolation, and specification decisions as on the underlying relationship. This highlights the importance of transparency in the selection and processing of rainfall data.

Keywords: Measurement errors, food insecurity, climate shocks, weather data, Sub-Saharan Africa
JEL Classification: Q54, O13, D12, I32

*I gratefully acknowledge the support of the Food and Agriculture Organization (FAO) through the "Open Science Research Grant" (Grant Agreement No. 04/2025 – SFER/GLO/501/MUL Baby 83). I would also like to thank Filippo Fossi, Julius Ssentongo, Amandine Poncin, Josselin Gauny, Neil Marsland, Anthony Ssebagereka, Bianca Tonetti, Ibrahim AliAhmad, Andrea Amparore, Alessia DeStefani, and others for their support in accessing the DEIM survey geocode, reviewing the draft, and providing valuable comments, suggestions, and feedback, as well as assisting with project coordination and budgeting. Their contributions were essential to the success of this research.

Corresponding author: `musahasen@gmail.com`

1 Introduction

Despite sustained global efforts, food insecurity remains a critical development challenge. In 2023, an estimated 28.9% of the world's population experienced moderate or severe food insecurity, with 864 million people suffering from severe hunger (FAO et al., 2024). The burden is disproportionately concentrated in Africa, where food insecurity rates are nearly twice the global average. Although Sustainable Development Goal 2 of the United Nations aims to eliminate hunger and malnutrition by 2030, current projections suggest that 582 million people will remain chronically undernourished, more than half of whom will reside in Africa.

Climate shocks such as drought compound these challenges by reducing agricultural yields, disrupting markets, and straining supply chains (Callahan & Mankin, 2022; Gregory et al., 2005; Mason-D'Croz et al., 2019; Zhang et al., 2023). These dynamics underscore the need for rigorous, data-driven strategies to enhance resilience. In particular, accurately measuring drought shocks is essential for understanding their impacts, informing effective policy design, and supporting strategies that strengthen adaptive capacity and long-term resilience. This is particularly true for Sub-Saharan Africa, as the vast majority of the population relies on climate-vulnerable sectors, such as agriculture, for their income, food, and livelihoods.

Among the common approaches to measuring drought shocks, self-reported indicators are widely used in household surveys. However, these measures are often vulnerable to errors arising from cognitive biases, recall limitations, and misperceptions. Respondents may misreport due to memory lapses, the salience of events, or confusion between genuine weather events and their coping ability. For example, rainfed farmers may overstate drought exposure, while more resilient households may underreport similar shocks. As Guiteras et al. (2015) note, salience bias can inflate reports of rare, extreme events, while repeated exposure may normalize shocks and lead to underreporting. These concerns are magnified when using binary indicators, where misclassification generates nonclassical measurement error (Abay et al., 2023; Meyer & Mittag, 2017).

To address these limitations, researchers increasingly turn to objective measures of rainfall variability. Advances in household survey technology, including GPS georeferencing and computer-assisted interviewing, now facilitate linking survey data with external rainfall records.[1] Among the available options, ground-based gauge measurements are widely regarded as the gold standard due to their rigorous quality control procedures and standardized measurement procedures (Josephson et al., 2026). Yet their coverage in Africa is extremely limited. The World Meteorological Organization reports that only 37 operational stations cover less than half of the continent's population, compared with more than 600 stations in the United States and European Union, which have a similar combined population (Tzachor et al., 2023). In Chad and Mali, for instance, fewer than ten Global Historical Climatology Network (GHCN) stations operate nationwide, as shown in Figure A1.[2]

In light of these gaps, researchers rely on satellite-based or reanalysis datasets to capture weather variability. These sources are relatively low-cost, widely accessible, and provide high spatial and temporal resolution rainfall values. However, they also present measurement challenges. For instance, satellite-based estimates are indirect, as they infer precipitation from signals such as cloud reflectance, infrared emissions, and microwave scattering (Alix-Garcia & Millimet, 2023). These methods may misclassify precipitation types or fail to detect light and short-duration events. As demonstrated by Jain (2020), these errors are often systematic and, if uncorrected, can bias statistical estimates. Reanalysis datasets, which integrate observational data with climate models, also present a different set of concerns. Their accuracy depends heavily on the

[1]These advances have also enabled the detection of measurement error in agricultural variables such as land size, input use, and crop yields (e.g., Abay, 2020; Abay et al., 2019, 2021; Dillon et al., 2019; Gourlay et al., 2019; Kosmowski et al., 2021; Wossen et al., 2019).

[2]The most recent station data were retrieved from the NOAA Global Historical Climatology Network (GHCN) dataset.

availability and quality of underlying observations, which are often scarce in low-income regions. Besides, reanalysis products tend to smooth extremes and misrepresent localized variability, especially in data-scarce environments. The spatial interpolation methods used in these models can also introduce artificial correlation patterns that distort local climate dynamics (Auffhammer et al., 2013).

Given that each dataset—whether satellite-based or reanalysis—differs in its methods of input processing, precipitation detection, and spatial and temporal resolution, they often capture different rainfall amounts. Consequently, the use of alternative rainfall datasets to measure drought shocks can yield divergent empirical results, even under identical research questions and analytical approaches. Such discrepancies weaken the reliability and comparability of findings, thereby affecting overall research quality. In some cases, they may also compel researchers to reconsider their choice of data source, raising concerns about selective reporting and, more broadly, the credibility of climate impact studies.

This study examines the extent to which the rainfall dataset choice influences estimates of the relationship between rainfall variability and food insecurity. I pursue two objectives. First, I assess how estimates of drought impacts differ across ten rainfall datasets. Using a consistent econometric specification, I estimate the association between Standardized Precipitation Index (SPI)-based drought measures and household food insecurity, and compare the sign, magnitude, and significance of coefficients across datasets. Second, I evaluate how spatial resolution and interpolation methods shape these results by systematically applying three approaches: zonal aggregation at the ADM3 level, nearest-neighbor interpolation, and bilinear interpolation.

I build on the work of Josephson et al. (2026), who examine how rainfall data choices affect estimates of agricultural productivity. While their focus is on production outcomes, I extend the analysis to food security, which provides a more direct measure of household welfare. In doing so, I contribute to the literature on measurement error in development economics. Most existing studies analyze mismeasurement in agricultural variables, such as land size (Abay et al., 2019, 2021), crop variety (Wossen et al., 2019), soil quality (Gourlay et al., 2019), and input use (Dillon et al., 2019; Kosmowski et al., 2021). Much less attention has been paid to weather data, despite its central role in climate–economics research. A few recent papers begin to address this gap (e.g., Alix-Garcia & Millimet, 2023; Fluhrer & Kraehnert, 2022; Gibson et al., 2021; Guiteras et al., 2015; Josephson et al., 2026), but none systematically evaluate how rainfall datasets shape estimates of drought impacts on food security. I aim to fill this gap by providing the first comprehensive assessment of how dataset choice and spatial processing influence estimates of rainfall shocks on household welfare.

The empirical analysis draws on nationally representative household survey data from Chad and Mali collected through the FAO's Data in Emergencies Monitoring (DIEM) system. These surveys are linked to rainfall data, with SPI computed for each dataset using a consistent historical reference period and a harmonized set of spatial methods. Food insecurity outcomes are then regressed on drought indicators using a uniform econometric model with a consistent set of controls.

The results show that estimates of rainfall variability's effect on food security are highly sensitive to both dataset choice and spatial interpolation. In specifications without controls, coefficients vary sharply in magnitude and sometimes reverse sign, reflecting omitted-variable bias compounded by measurement error, aggregation, and resolution. Once controls are introduced, this heterogeneity largely disappears. Within-method variation is modest, and cross-method differences shrink substantially, indicating that much of the instability in uncontrolled models reflects unobserved confounders rather than genuine spatial heterogeneity. Regarding the interpolation techniques, bilinear interpolation yields moderate and stable estimates, nearest-neighbor assignments that were initially volatile converge toward reliability, and zonal aggregation produces the largest coefficients by averaging within-region variation.

While our study primarily focuses on food insecurity, the datasets we employ have broad applicability across diverse research fields and analytical scales. They have been instrumental in research examining the effects of weather on agricultural productivity (Deschênes & Greenstone, 2007; Jagnani et al., 2021), education (Colmer, 2021; Fishman et al., 2019; Maccini & Yang, 2009; Rosales-Rueda, 2018), health outcomes (Banerjee & Maharaj, 2020; M. Burke et al., 2015; Cooper et al., 2019; Dinkelman, 2017), family dynamics and demographic trends (Corno et al., 2020; Rocha & Soares, 2015), labor market behavior (Branco & Féres, 2021; Feeny et al., 2021; Jayachandran, 2006), migration (Gröger & Zylberberg, 2016), conflict (Harari & Ferrara, 2018), firm-level productivity (Bas & Paunov, 2025), and macroeconomic indicators (Carleton & Hsiang, 2016). Given their widespread use, our study's findings, which underscore the limitations of these datasets, are essential for advancing empirical research in these domains.

The remainder of the paper is structured as follows. Section 2 describes the data sources, including household surveys and rainfall datasets. Section 3 outlines the empirical strategy. Section 4 presents and discuss the results of the study. Section 5 concludes with implications for policy and future research.

2 Data

2.1 Household Survey: DIEM data

I draw on household-level data from the Food and Agriculture Organization's (FAO) Data in Emergencies Monitoring (DIEM) system to construct the food security outcome variable and covariates. Launched in June 2020, DIEM provides high-frequency data to monitor the impacts of shocks on food security and agricultural livelihoods in crisis-affected settings. The survey follows a harmonized design across countries and includes detailed modules on demographics, food security status, and household exposure to recent shocks (Amparore et al., 2023).

For this study, I use DIEM data from Chad (Rounds 6–8, collected between January 2024 and February 2025) and Mali (Round 7, collected in January 2024). These countries are selected due to data availability, including geocoded household locations, as well as their high prevalence of poverty, food insecurity, and dependence on rainfall in the face of growing climate variability. Chad, for example, ranks 187th of 189 countries on the Human Development Index and has been classified as fragile since 2006. In 2022, 44.8% of the population lived below the national poverty line, and by 2024, the share of people in extreme poverty ($2.15/day, 2017 PPP) had risen to 36.5%. The country also ranks among the five most climate-vulnerable globally (World Bank, 2023, 2025a). Mali faces similar challenges (World Bank, 2022, 2025b). Extreme poverty increased from 15.9% in 2021 to 19.1% in 2022, driven by security crises, the COVID-19 pandemic, rising prices, and weak growth. In both countries, the majority of households live in rural areas and rely heavily on agriculture, making rainfall variability a critical threat to food security and livelihoods.

I use the Food Insecurity Experience Scale (FIES) as a proxy for food security. The FIES captures both access constraints and the psychological stress of uncertainty, providing a direct and internationally comparable measure of households' lived experiences of food insecurity. By reflecting insufficiency, uncertainty, and deprivation, it is particularly well-suited for evaluating the welfare consequences of climate shocks. The FIES is based on eight questions that capture households' experiences and behaviors when facing constraints in accessing sufficient food. These questions encompass concerns about food availability, compromises in dietary quality, and reductions in food intake, thereby enabling a comprehensive assessment of food insecurity. Table B3 in the Appendix summarizes household responses to each question. Using these raw responses, I calculate food insecurity levels through Rasch model estimates, following the FAO methodology.[3] The model provides thresholds for moderate and severe food insecurity. These measures capture both the intensity and prevalence of food insecurity, and I use them as outcome indicators in the empirical analysis. It is also important to underscore that the objective of this paper is not to re-estimate the average effect of rainfall variability on food security, which is well established, but rather to assess how estimated impacts of drought shock on food insecurity vary across rainfall datasets and interpolation methods.

2.2 Weather Data and Construction of Drought Indicator

Ten publicly available rainfall datasets that vary in modeling approaches, input sources, and spatial resolution are used for this study. To ensure consistency and comparability, datasets with a minimum record length of 20 years, extending at least through the earliest DIEM survey rounds, are selected. A brief overview of these datasets is provided below.

- **CHIRPS:** The Climate Hazards Group InfraRed Precipitation with Stations dataset provides quasi-global rainfall estimates from 1981 to the present at a fine spatial resolution of 0.05°. The dataset is available in daily, pentadal (5-day), and monthly formats. CHIRPS is developed by the Climate Hazards Center at the University of California, Santa Barbara. It combines satellite-derived Cold Cloud Duration (CCD) data with in-situ rain gauge observations, producing a hybrid product that balances spatial coverage and accuracy (Funk et al., 2015). CHIRPS is widely used across disciplines, including agriculture and household welfare (Amare & Balana, 2023; Baysan et al., 2024; Miguel, 2024), conservation and climate resilience (Michler et al., 2019), child nutrition and health (Di Falco & Han, 2025; Omiat & Shively, 2020), fertility decisions and marriage outcomes (Fontaine et al., 2024; Hotte & Lambert, 2023), and conflict-related studies (Sakketa et al., 2025).

- **CMAP:** CPC Merged Analysis of Precipitation (CMAP) is developed by the Climate Prediction Center at the National Oceanic and Atmospheric Administration (NOAA), and provides global precipitation estimates from 1979 to the present at a spatial resolution of 2.5° × 2.5°, available in monthly and pentadal formats. The dataset merges satellite-derived precipitation products with in-situ rain gauge observations through optimal interpolation techniques. CMAP is widely employed in climate risk assessments, environmental economics studies, conflict analysis, and public health research (e.g., Garg et al. (2018), Gu et al. (2024), Hsiang et al. (2011) and Michler et al. (2022)), where it often serves as a key explanatory variable or a control for weather and climate effects.

- **CRU TS:** Climatic Research Unit Time-Series (CRU TS) is developed by the Climatic Research Unit at the University of East Anglia. Unlike satellite-derived datasets, CRU TS relies exclusively on ground-based measurements from national meteorological services, global archives, and international organizations. It provides monthly precipitation data at a spatial resolution of 0.5° × 0.5° for all terrestrial areas except Antarctica, with records extending back to 1901 (Harris et al., 2020). CRU TS is extensively used in studies of climate variability, hydrological modeling, agricultural productivity, and economic development (e.g., Emediegwu et al., 2022; Felbermayr et al., 2022; Freudenreich et al., 2022; Hazrana et al., 2025; Kalkuhl & Wenz, 2020; Ricker-Gilbert & Jones, 2015; Sekhri & Storeygard, 2014; Van der Merwe et al., 2022).

[3] See the online computation tool at https://fies.shinyapps.io/ExtendedApp/.

- **ERA5:** ECMWF Reanalysis v5 (ERA5) is produced by the European Centre for Medium-Range Weather Forecasts (ECMWF) under the Copernicus Climate Change Service. It offers hourly estimates of a broad range of climate variables, including rainfall and temperature, from 1950 to the present at a spatial resolution of $0.25^\circ \times 0.25^\circ$. ERA5 combines numerical weather prediction models with extensive observational data using advanced data assimilation techniques (Hersbach et al., 2020). The dataset is widely employed in empirical research across disciplines, including (Azzarri & Nico, 2022; Dasgupta & Robinson, 2023; Flores et al., 2024; Jagnani et al., 2021; Sedova & Kalkuhl, 2020; Ubilava et al., 2023).

- **GPCP:** Global Precipitation Climatology Project (GPCP) is developed under the World Climate Research Programme. It provides global monthly precipitation estimates from January 1979 to the present at a spatial resolution of $2.5^\circ \times 2.5^\circ$ (Adler et al., 2003; Huffman et al., 2001). It merges multiple observational sources using a calibrated weighting algorithm that corrects frequent infrared estimates with the more accurate but temporally sparse microwave data. Studies that used the GPCP dataset include M. B. Burke et al. (2009), Mueller & Seneviratne (2012) and Sheffield et al. (2006).

- **NCEP–DOE AMIP-II Reanalysis (R-2):** Developed collaboratively by the National Centers for Environmental Prediction (NCEP) and the Department of Energy (DOE), the NCEP–DOE AMIP-II Reanalysis (R-2) is a reanalysis product spanning 1979 to the present at $2.5^\circ \times 2.5^\circ$ spatial resolution(Kanamitsu et al., 2002). R-2 builds upon the NCEP–NCAR Reanalysis (R-1), addressing its limitations, including human processing errors, model deficiencies, and diagnostic shortcomings. The project incorporates an updated forecast model, an improved data assimilation system, and a comprehensive set of diagnostic outputs, effectively correcting errors identified in R-1. R-2 assimilates both ground-based observations and satellite measurements. Studies that used this dataset include Jolly et al. (2015), Minor et al. (2022), Obradovich et al. (2017), Russo et al. (2017) and Schwalm et al. (2017).

- **PREC/L**: NOAA Precipitation Reconstruction Over Land (PREC/L) is developed by NOAA's Climate Prediction Center. It provides a global analysis of monthly precipitation from 1948 to the present (Chen et al., 2002). Land precipitation is generated through Optimal Interpolation of observations from over 17,000 gauge stations in the NOAA/NCEI Global Historical Climatology Network (GHCN v2) and the NOAA/CPC Climate Anomaly Monitoring System (CAMS) (Physical Sciences Laboratory, n.d.). PREC/L offers three spatial resolutions ($2.5^\circ \times 2.5^\circ$, $1^\circ \times 1^\circ$, $0.5^\circ \times 0.5^\circ$) and captures mean precipitation patterns, seasonal cycles, and ENSO-related anomalies. Studies that used this dataset include (Huang et al., 2016; Kang et al., 2021; Smith et al., 2023).

- **PERSIANN PDIR-Now**: Precipitation Estimation from Remotely Sensed Information using Artificial Neural Networks – Precipitation Data & Information for Nowcasting (PERSIANN PDIR-Now) is developed by the Center for Hydrometeorology and Remote Sensing at the University of California. PERSIANN PDIR-Now is a near-real-time, global precipitation dataset providing hourly rainfall estimates at $0.04^\circ \times 0.04^\circ$ spatial resolution across latitudes 60°S to 60°N (Nguyen et al., 2020). PERSIANN PDIR-Now is a satellite-based precipitation dataset that estimates rainfall in near real-time using infrared observations from geostationary satellites and artificial neural networks to derive precipitation intensity (Nguyen et al., 2020; Sorooshian et al., 2000).

- **TAMSAT:** Tropical Applications of Meteorology using Satellite and ground-based observations (TAMSAT) is developed by the University of Reading. It provides satellite-based rainfall estimates across

Africa and tropical regions by analyzing Cold Cloud Duration from Meteosat infrared imagery, calibrated with ground rain gauge data (Maidment et al., 2014). It delivers high spatial resolution precipitation data at approximately 0.0375° × 0.0375°, with temporal resolutions including daily, 5-day, 10-day, monthly, and seasonal aggregates, covering the period from 1983 to the present. The dataset is widely used for climate monitoring, agricultural applications, and drought risk management (Chamberlin & Ricker-Gilbert, 2016; Eberhard-Ruiz & Moradi, 2019; Fischer et al., 2019; Harrison et al., 2019; Leroux et al., 2019; Wagner et al., 2024).

- **TerraClimate:** TerraClimate is a high-resolution (0.04°) global dataset that provides monthly climate and water balance data for terrestrial surfaces from 1958 onward (Abatzoglou et al., 2018). It combines climatological normals from WorldClim with time-varying data from the Climatic Research Unit Time-Series (CRU TS) and the Japanese 55-year Reanalysis (JRA-55).

As a demonstration, the rainfall conditions across Chad in a particular month, captured by the ten identified precipitation datasets, are shown in Figure 1. This visual comparison highlights the spatial and quantitative variability among the datasets, despite representing the same month and geographic area.

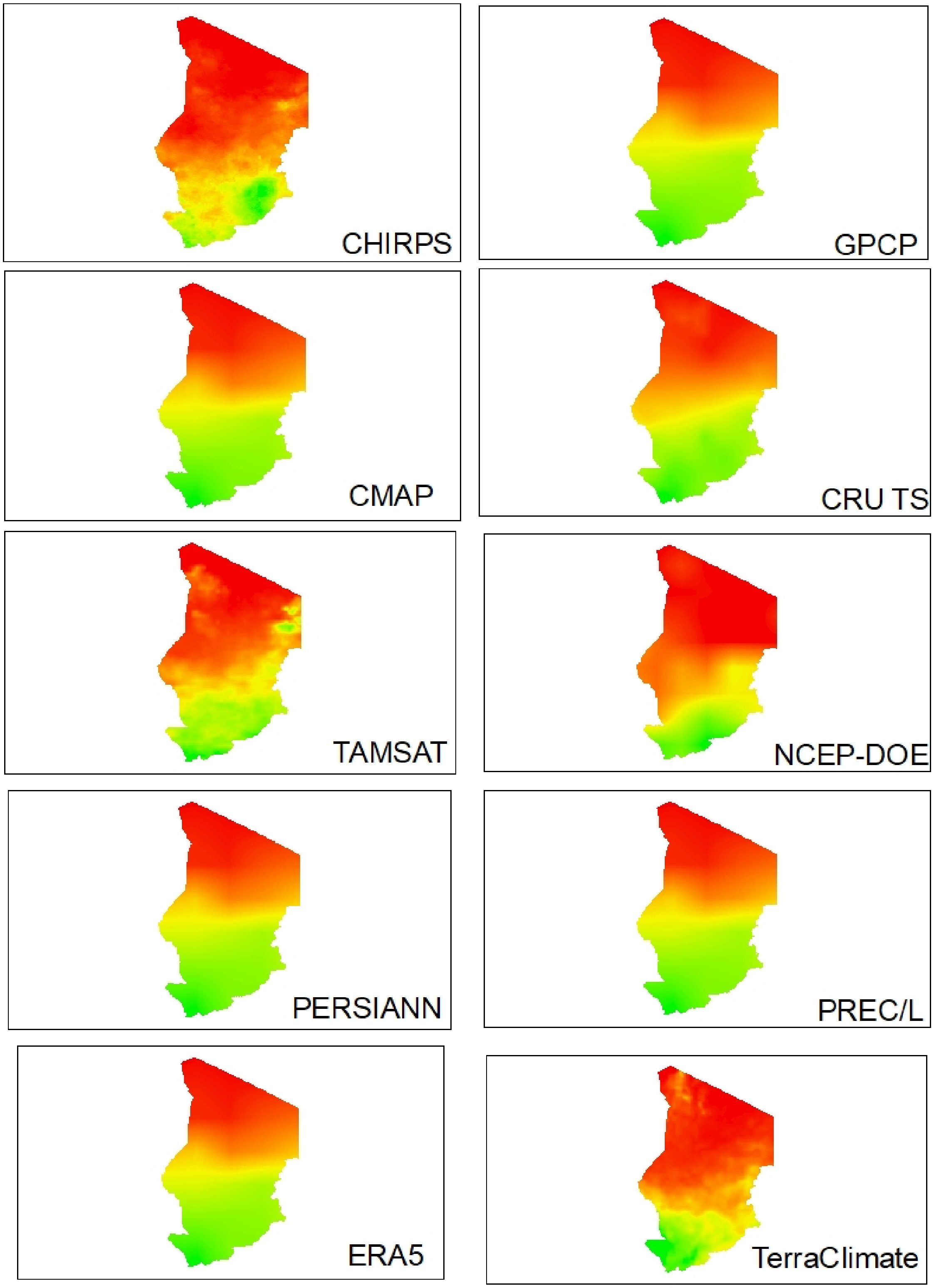

Figure 1: Comparison of Rainfall Estimates from Multiple Precipitation Products – Chad, August 2023

Source: Author's illustration. The figure shows rainfall measurements from all ten precipitation products for Chad during August 2023.

Using the selected weather datasets, I construct a drought indicator based on the Standardized Precipitation Index (SPI), a widely adopted measure in economic and environmental research for assessing drought conditions (McKee et al., 1993). The SPI quantifies deviations of observed precipitation from its long-term historical distribution, enabling consistent comparisons of drought severity across both space and time. The SPI values below zero indicate drier-than-normal conditions, while values above zero represent wetter-than-normal periods. Hence, the SPI enables robust cross-regional and temporal drought assessments within a consistent statistical framework.

To account for the typically skewed and non-negative nature of precipitation data, I model the historical precipitation series using a gamma probability distribution, which provides a flexible and empirically appropriate representation of rainfall variability. To maintain comparability, I apply a uniform historical reference period for the estimation of the gamma parameters and subsequent SPI computation.

2.3 Merging DIEM and Weather Datasets

I obtained the geolocations of households from the DIEM team. To protect respondent anonymity, the team intentionally displaced each location within a 1.1 km radius, which is considerably smaller than the standard 5 km offset applied to publicly available LSMS or DHS data in rural areas. Although such spatial displacement may introduce potential misalignment between household locations and the rainfall datasets, Michler et al., 2022 show that even the larger LSMS displacement has minimal impact on such empirical results. Given this evidence, the finer displacement in DIEM is unlikely to introduce significant bias in the analysis.

To integrate DIEM household data with the gridded weather variables, I implement three spatial interpolation methods: bilinear interpolation, nearest-neighbor matching, and zonal averaging based on third-level administrative units (ADM3). Each method addresses the trade-off between spatial accuracy and noise differently. Bilinear interpolation estimates values at the household point by taking a weighted average of the four nearest grid cells, providing smooth spatial transitions but potentially attenuating local extremes. Nearest-neighbor matching assigns each household the value of the closest grid cell, thereby preserving the original gridded values. However, this approach may perform poorly for datasets with coarse spatial resolution, since the nearest grid cell may still be far from the household's true location. Zonal averaging aggregates weather variables at the ADM3 level and assigns each household the mean value of its administrative unit, thereby reducing random spatial measurement error. However, this method may obscure within-zone heterogeneity, and because ADM3 boundaries are politically defined, their size and shape vary considerably, leading to unequal aggregation units across space.

3 Estimation Strategy

I employ a consistent econometric framework across all datasets to estimate the effects of drought on food security outcomes and to examine whether different weather data sources and interpolation techniques yield systematically stronger or weaker estimates. The analysis compares both the magnitude and statistical significance of drought coefficients across specifications and visualizes the results using specification charts, which display estimated coefficients and their confidence intervals for each model variant. The empirical strategy follows the regression sequence below:

$$Y_{ht} = \beta_0 + \beta_1 \omega_{ht} + \varepsilon_{ht} \tag{1a}$$

$$Y_{ht} = \beta_0 + \beta_1 \omega_{ht} + \delta_j K_{jht} + \varepsilon_{ht} \tag{1b}$$

Here, Y_{ht} denotes the food security outcome for household h in period t. The key explanatory variable, ω_{ht}, represents the Standardized Precipitation Index derived from the datasets described in Section 2.2.

Model (1a) estimates the unconditional relationship between drought and food security outcomes. Model (1b) extends this specification by including a vector of household-level covariates, K_{jht}. Careful attention is given to the inclusion of control variables, as climate shocks can influence many factors that might otherwise be considered controls. To mitigate potential "bad control" bias, only variables plausibly exogenous to drought are included. These controls capture factors such as, human capital (e.g., educational attainment), and demographic characteristics (e.g., household size, gender, and age of the household head). I also included survey round fixed effects, controls for seasonality (to account for within-year variation in food security), and country fixed effects.

As a robustness exercise, I further control for household exposure to multiple types of shocks—including economic, agricultural, environmental, conflict-related, and idiosyncratic shocks. These are excluded from the main specification since they are expected to be highly correlated with drought exposure. The robustness analysis also incorporates factors that may mediate or buffer the impacts of drought, such as access to formal and informal social protection (e.g., cash transfers, NGO support) and coping mechanisms like irrigation infrastructure, which enhances resilience by reducing dependence on rainfall. The results of these robustness tests are presented in Appendix Figure A2.

4 Results and Discussions

4.1 Descriptive statistics for Working Variables

This sub-section presents and discusses the working variables used in the analysis. Table 1 reports descriptive statistics for the outcome and control variables extracted from DIEM. As shown in the table, the sample is predominantly male-headed, with 76% of households headed by men. This share is significantly higher in Mali (90%) than in Chad (74%). Educational attainment remains low across the sample, as 55% of household heads have no formal primary education, with similar levels in Chad (55%) and slightly higher rates in Mali (58%). Regarding agricultural production roles, crop farming dominates respondents' livelihoods, with 82% identifying as crop producers. The proportion is higher in Chad (84%) than in Mali (67%). Livestock production is also common, with 52% of respondents engaged in it, showing modest variation across countries. Fish production is rare overall (9%), especially in Mali, where only 1% of households report engaging in it, compared to 10% in Chad. Irrigation use is limited, with just 4% of households using any form of irrigation. The contrast between countries is substantial, as only 2% of households in Chad report irrigation use, compared to 17% in Mali.

Shock exposure is widespread across the sample. Approximately 80% of households report experiencing at least one shock in the past year, with a slightly higher prevalence in Chad (80%) than in Mali (78%). Economic shocks are the most common type, affecting 54% of households in Chad and 34% in Mali. Agricultural and environmental shocks are also more prevalent in Chad (28% and 26%, respectively) than in Mali (14% and 12%). By contrast, conflict-related shocks are notably more frequent in Mali, affecting 22% of households compared to just 7% in Chad, consistent with Mali's ongoing security crisis during the survey period. Household-level shocks, such as illness or death, affect around 43% of the pooled sample, with little difference between countries. Despite the high incidence of shocks, only about 13–15% of households report receiving any assistance. Food insecurity is also more severe in Chad, as about 63% of households experience moderate to severe food insecurity, compared to 43% in Mali.

Table 1: Summary statistics of key household variables in pooled sample and by country

Variable	**Pooled (n=16,423)**		**Chad (n=14,503)**		**Mali (n=1,920)**	
	Mean	Std. Dev.	Mean	Std. Dev.	Mean	Std. Dev.
Household head is male	0.76	0.43	0.74	0.44	0.90	0.30
No primary education (HH head)	0.55	0.50	0.55	0.50	0.58	0.49
Household head age (quartile)	2.68	0.63	2.62	0.60	2.92	0.69
Respondent is livestock producer	0.52	0.50	0.52	0.50	0.57	0.50
Respondent is crop producer	0.82	0.38	0.84	0.37	0.67	0.47
Respondent is fish producer	0.09	0.28	0.10	0.30	0.01	0.12
Household uses irrigation	0.04	0.19	0.02	0.14	0.17	0.37
Experienced any shock	0.80	0.40	0.80	0.40	0.78	0.41
Household-related shocks	0.43	0.49	0.43	0.50	0.40	0.49
Economic shock	0.51	0.50	0.54	0.50	0.34	0.47
Agricultural shock	0.26	0.44	0.28	0.45	0.14	0.34
Environmental shock	0.25	0.43	0.26	0.44	0.12	0.32
Conflict-related shock	0.09	0.29	0.07	0.26	0.22	0.42
Received any assistance	0.13	0.34	0.13	0.34	0.15	0.36
Lean season	0.06	0.25	0.07	0.26	0.00	0.00
Rainy season	0.26	0.44	0.30	0.46	0.00	0.00
Peak season	0.67	0.47	0.63	0.48	1.00	0.00
Moderate or Severe food insecurity experience	0.61	0.41	0.63	0.40	0.39	0.43

Turning to the rainfall data, Figures 2–4 present correlation matrices of rainfall estimates from 2003 to 2024 obtained using three spatial interpolation techniques: nearest neighbor, bilinear, and zonal averaging at the ADM3 level. Across all methods, the correlations among gauge-based and hybrid products remain consistently high, often exceeding 0.90. For instance, CHIRPS, GPCP, PREC_L, and TAMSAT exhibit particularly strong pairwise correlations, with CHIRPS–GPCP consistently at 0.97–0.98 across interpolation schemes. These findings highlight the robustness of hybrid datasets that combine dense gauge inputs with satellite retrievals, which maintain strong alignment regardless of the spatial processing method.

By contrast, coarse resolution reanalysis products, especially NCEP_DOE, show systematically weaker correlations with higher resolution datasets. Under bilinear interpolation, NCEP_DOE correlates only 0.70–0.78 with gauge-based products, and as low as 0.61 with TerraClimate. Nearest neighbor interpolation further exacerbates the divergence, with NCEP_DOE–CHIRPS at 0.73 and NCEP_DOE–TerraClimate at 0.62. Even when smoothed through zonal averaging, which raises NCEP_DOE–CHIRPS correlations to about 0.77 and with TerraClimate to 0.64, the dataset remains an outlier. This pattern illustrates how coarse grid structures amplify misalignment when matched to fine scale household locations, introducing spatial mismatch and artificial noise. PERSIANN_CDR, while higher resolution, also displays weaker alignment with gauge-based products (0.83–0.90), reflecting systematic biases in satellite-only retrievals.

Interpolation choice itself exerts a nontrivial influence on correlation magnitudes. Zonal averaging produces the highest coefficients overall, particularly bridging gaps between coarse reanalysis datasets and fine resolution gauge-based products. For example, ERA5–CHIRPS correlations rise from 0.88 under bilinear interpolation to 0.92 under zonal averaging, suggesting that aggregation smooths local discrepancies and attenuates measurement noise. Bilinear interpolation maintains robust correlations but preserves more local variation, which slightly reduces coefficients relative to zonal averaging. Nearest neighbor, however, performs worst in reconciling mismatched resolutions: correlations involving coarse datasets (e.g., NCEP_DOE) fall to their lowest levels under this method, confirming that nearest neighbor assignment is ill suited for analyses requiring household-level precision.

These results show that dataset resolution and spatial processing interact to shape the apparent consistency of rainfall measures. High resolution hybrid datasets remain stable across methods, while coarse reanalyses are highly sensitive to interpolation choices. This reinforces the need for alignment between dataset resolution, interpolation strategy, and research design in climate and economics applications.

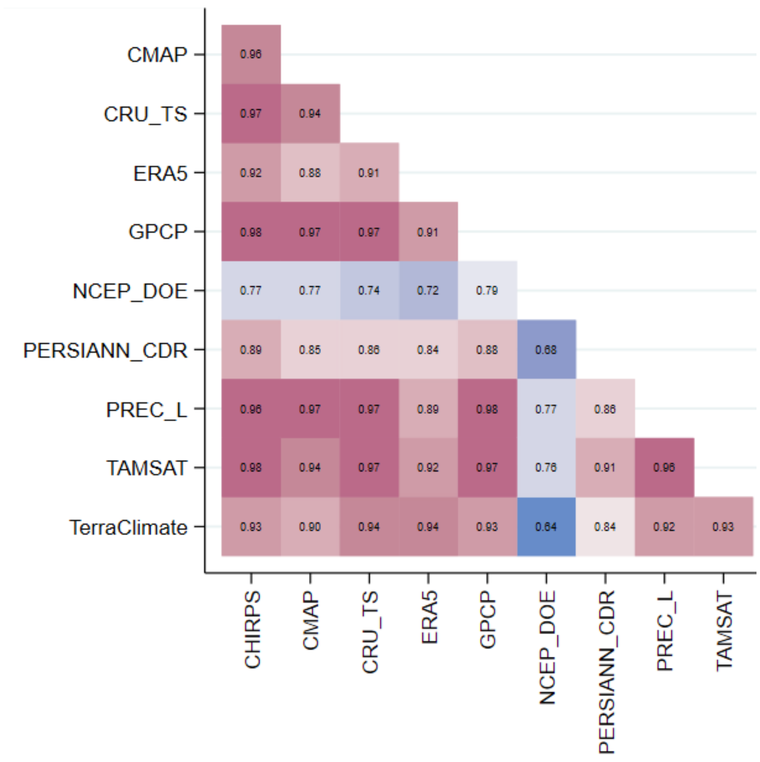

Figure 2: Correlation matrix of rainfall estimates using Zonal averaging (ADM3).

Using the rainfall estimates obtained from the three interpolation techniques, I compute the SPI for each dataset based on the Gamma distribution. Table 2 summarizes the resulting SPI values across datasets for Bilinear (BL), Zonal averaging (Zone), and Nearest-Neighbor (NN) interpolation. Across datasets, mean SPI values vary substantially, reflecting differences in precipitation retrieval algorithms, gauge corrections, and spatial resolutions. In contrast, within each dataset, the choice of interpolation method yields only marginal shifts in both mean and standard deviation, suggesting that dataset-specific characteristics, rather than spatial interpolation, are the dominant source of variation in drought indicators.

Gauge-calibrated and high-resolution products such as CHIRPS and CRU TS exhibit remarkable consistency across interpolation methods. For instance, CHIRPS records mean SPI values of 1.07 (BL), 1.05 (Zone), and 1.06 (NN), while CRU TS remains stable around 0.49 under all three approaches. This stability highlights the robustness of these datasets to spatial processing. In contrast, coarse-resolution datasets show greater sensitivity. CMAP, which operates on a 2.5° grid, records a mean SPI of 1.38 under BL but declines to 1.20 under Zone and 1.27 under NN, underscoring the role of resolution and spatial aggregation in shaping drought indices.

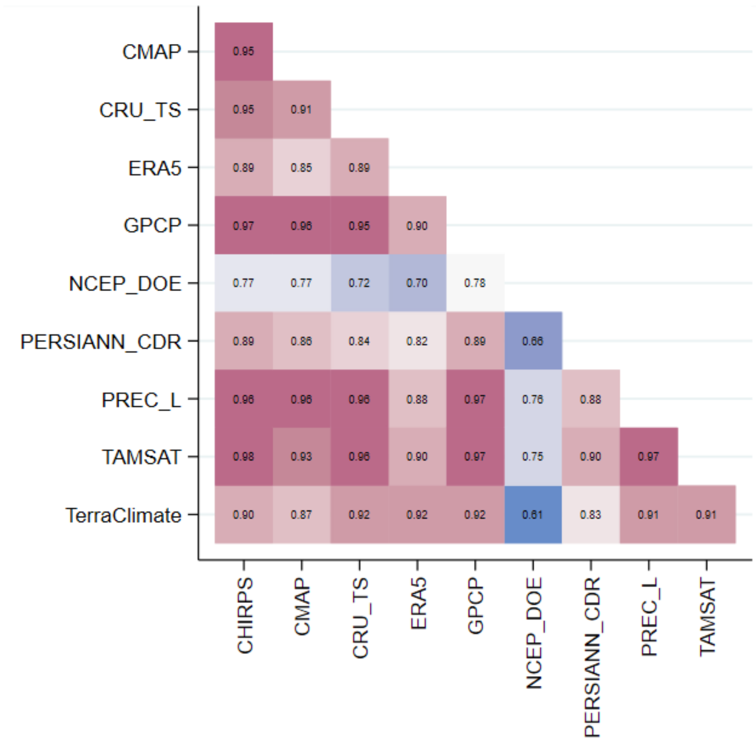

Figure 3: Correlation matrix of rainfall estimates using Bilinear interpolation.

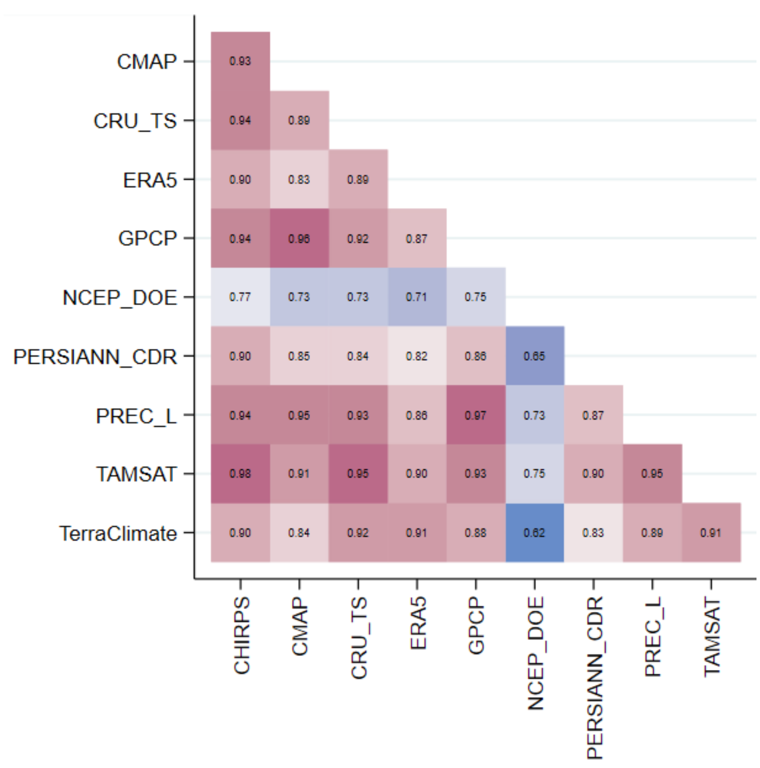

Figure 4: Correlation matrix of rainfall estimates using Nearest neighbor interpolation.

ERA5 displays consistently negative mean SPI values (ranging from −0.67 to −0.69) and the highest variability (SD ≈ 2.36–2.40), indicating that its reanalysis-based precipitation fields may overstate interannual fluctuations relative to gauge-calibrated products. NCEP_DOE similarly centers near zero but shows moderate sensitivity to the interpolation scheme. Among satellite-only datasets, PERSIANN_CDR produces comparable means (≈ 0.34) and standard deviations (≈ 0.89–0.90) across methods, while PREC_L shows a clear decline under Zonal averaging (mean = 0.73) compared to BL (0.96), implying that aggregation smooths local extremes. TAMSAT remains particularly stable (means ≈ 0.83–0.86), and TerraClimate exhibits a consistent negative bias (≈ −0.27) with substantial dispersion (SD ≈ 1.67–1.69).

From a methodological perspective, Bilinear interpolation generally yields slightly higher mean SPI values for coarse datasets, owing to its smoothing effect across adjacent grid cells. Nearest-Neighbor tends to marginally reduce variability by preserving original grid-point values, though at the expense of continuity. Zonal averaging occupies an intermediate position, dampening spatial noise but potentially obscuring localized drought or excess-rainfall anomalies.

Table 2: Summary Statistics of SPI by Interpolation Method

Dataset	**Bilinear (BL)**		**Zone**		**Nearest Neighbour (NN)**	
	Mean	SD	Mean	SD	Mean	SD
CHIRPS	1.07	0.85	1.05	0.90	1.06	0.85
CMAP	1.38	1.10	1.20	1.23	1.27	1.12
CRU TS	0.49	1.13	0.49	1.13	0.49	1.13
ERA5	−0.67	2.36	−0.69	2.40	−0.67	2.36
GPCP	0.71	0.91	0.71	0.89	0.69	0.91
NCEP_DOE	0.00	0.97	0.01	0.93	0.04	0.96
PERSIANN_CDR	0.34	0.89	0.34	0.90	0.34	0.89
PREC_L	0.96	1.06	0.73	1.24	0.92	1.10
TAMSAT	0.86	0.85	0.83	0.86	0.85	0.85
TerraClimate	−0.27	1.67	−0.24	1.69	−0.27	1.67

After computing the SPI, I examined its statistical relationship with subjective drought reports from the DIEM survey and with household income. These analyses serve as validation exercises, illustrating how effectively different precipitation datasets capture real-world drought experiences and economic outcomes.

Table B1 reports the correlations between self-reported drought shocks and SPI values derived from precipitation estimates fitted to a Gamma distribution. Across datasets, the correlations are consistently negative and highly significant, confirming that wetter conditions (higher SPI) are associated with lower reported drought incidence. The strongest associations are observed for CHIRPS, CMAP, TerraClimate, and PREC/L, all of which rely on dense gauge networks or hybrid methods that integrate satellite and observational data. ERA5 and CRU TS show moderate alignment with household perceptions, while TAMSAT and PERSIANN-CDR display weaker correlations. GPCP performs relatively poorly, and NCEP-DOE remains close to zero, indicating limited correspondence with subjective drought experience. Importantly, the choice of interpolation method has minimal effect on these patterns, implying that dataset construction rather than resampling explains the observed variation.

I also analyzed the association between rainfall conditions and household income to assess the extent to which rainfall variability influences welfare outcomes through production, labor markets, and local price channels. The results, presented in Table B2, indicate that rainfall shocks are generally positively correlated with total household income, consistent with the high dependence of rural livelihoods on rainfall availability.

The strongest correlations are found for CRU TS and NCEP-DOE, which capture broad rainfall–income linkages despite their coarse resolution. Hybrid datasets such as CHIRPS, TerraClimate, and PREC/L also exhibit meaningful positive associations, while TAMSAT and PERSIANN-CDR show weaker and less stable relationships, reflecting the limitations of satellite-only retrievals. Notably, CMAP and PREC/L exhibit sign reversals under zonal averaging, suggesting that spatial aggregation can obscure or distort local rainfall–income sensitivities.

Taken together, these findings demonstrate that while most rainfall datasets reproduce the expected relationships between climatic conditions, perceived drought, and household income, their performance varies systematically with gauge reliance, resolution, and construction method. Dataset characteristics, rather than interpolation techniques, are the primary determinants of their ability to align with household-level outcomes.

4.2 Econometrics Results

The estimation of rainfall variability effects on household food insecurity using the ten rainfall datasets, under three spatial interpolation techniques and without controls, reveals substantial heterogeneity across products and methods. Across all interpolation schemes, both the magnitude and direction of coefficients vary, indicating that dataset characteristics and spatial processing significantly shape estimated relationships.

Under bilinear interpolation (Figure 5a), estimated coefficients range from approximately −0.06 for NCEP–DOE to +0.02 for PERSIANN–CDR. The nearest-neighbour method (Figu[illegible]-parable pattern, with coefficients spanning from about −0.05 for NCEP–DOE to +[illegible] PERSIANN–CDR. The zonal aggregation approach (Figure 5c) yields the widest [illegible] extending from roughly −0.06 for NCEP–DOE to +0.04 for PREC/L.

Could there be a positive bias linked to urban areas - where perhaps more signals (microwaves, reflections) are mistaken for rain correlate with higher food security in urban areas?

Dataset-specific responses also shift notably across interpolation techniques. [illegible] changes from around +0.02 under nearest-neighbour to approximately +0.01 under z[illegible] PREC/L transitions from slightly negative (−0.01) under bilinear and nearest-neighbour to strongly positive (+0.04) under zonal aggregation. Conversely, CHIRPS consistently yields negative coefficients, generally between −0.02 and −0.03, though magnitudes differ slightly by method. NCEP–DOE exhibits the most consistent and pronounced negative association (roughly −0.05 to −0.06), unaffected by interpolation, indicating strong sensitivity of food insecurity to rainfall deficits in this dataset.

Resolution and data source play key roles in explaining these patterns. High-resolution blended datasets such as CHIRPS and TerraClimate consistently produce negative coefficients, aligning with expectations that increased rainfall reduces food insecurity. Their fine spatial representation and gauge calibration enhance stability across interpolation techniques. Gauge-based datasets like CRU TS remain relatively robust, typically around −0.03, reflecting their long observational record. In contrast, coarse global products such as CMAP and PREC/L show high sensitivity to interpolation, with coefficient signs reversing between bilinear or nearest-neighbour and zonal aggregation.

Satellite-only datasets, including TAMSAT and PERSIANN–CDR, frequently produce positive coefficients under bilinear and nearest-neighbour interpolation, suggesting potential biases in rainfall detection or spatial averaging that inflate estimated food insecurity risk with increasing rainfall. These effects largely dissipate when zonal aggregation is applied, bringing coefficients closer to zero. Among the reanalysis products, NCEP–DOE remains strongly negative across all methods, while ERA5 yields small, stable coefficients near zero, consistent with its finer resolution and reliance on model dynamics.

A distinct structural pattern emerges once controls are introduced (Figures 6). Across interpolation methods, estimated coefficients converge toward consistently negative values, consistent with theoretical

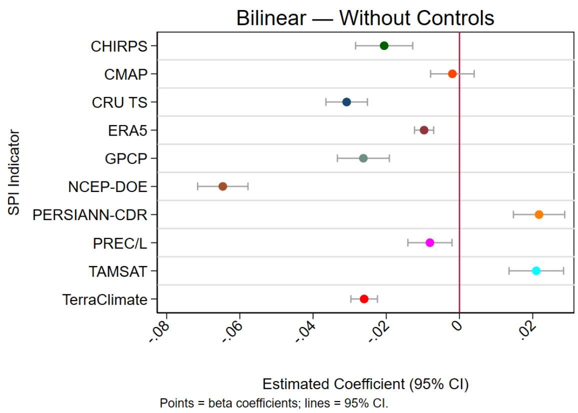

(a) Bilinear interpolation coefficients.

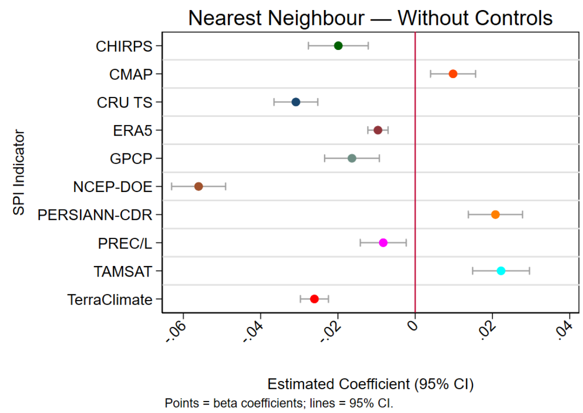

(b) Nearest-neighbor interpolation coefficients.

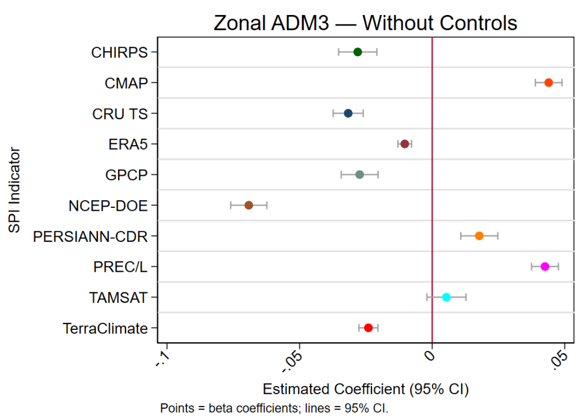

(c) Zonal aggregation coefficients.

Figure 5: Estimated coefficients without controls across interpolation methods.

expectations that higher rainfall alleviates food insecurity. The inclusion of controls substantially reduces both within-method dispersion and cross-dataset instability, suggesting that much of the heterogeneity in the uncontrolled models reflected omitted-variable bias rather than genuine spatial differences in rainfall exposure.

Under bilinear interpolation, coefficients range from –0.057 (TerraClimate, NCEP–DOE) to –0.004 (TAMSAT). Nearest-neighbour interpolation, previously the most volatile, now yields uniformly negative estimates between –0.057 (TerraClimate) and –0.002 (TAMSAT). Zonal aggregation continues to produce the largest-magnitude effects (NCEP–DOE: –0.061; TerraClimate: –0.053; CHIRPS: –0.047), though the overall spread of coefficients narrows sharply relative to the uncontrolled models.

Differences across datasets can be traced to their underlying spatial resolution and construction features. High-resolution blended products such as CHIRPS and TerraClimate produce strong and statistically significant coefficients (–0.047 to –0.057), reflecting their capacity to capture localized rainfall shocks relevant for household production and consumption dynamics. Gauge-based products such as CRU TS yield moderately negative but stable coefficients (–0.028 to –0.034), consistent with the reliability of long-term station records.

By contrast, coarser datasets such as CMAP (2.5°) and PREC/L (2.5°) remain more sensitive to interpolation. Although the inclusion of controls renders their coefficients consistently negative, magnitudes are smaller and less stable across methods (–0.014 to –0.031), highlighting the difficulty of identifying micro-level impacts from aggregated rainfall measures. Satellite-only datasets (TAMSAT and PERSIANN–CDR) continue to behave as outliers: even after controlling for confounders, their coefficients remain weak and close to zero (–0.004 to –0.019), underscoring the limitations of infrared-only retrievals for fine-scale socioeconomic analysis.

Reanalysis datasets exhibit further divergence. NCEP–DOE produces the most negative and stable coefficients (–0.057 to –0.061), while ERA5 yields smaller but consistently negative effects (–0.009 to –0.013). These differences likely reflect distinct data assimilation systems and gauge correction schemes, with coarser-resolution NCEP emphasizing rainfall variability in a way that maps more directly onto household outcomes.

A related finding concerns the instability of *ordinality*, the relative ranking of rainfall datasets, across interpolation methods and model specifications (Figures 5 and 6). In the uncontrolled models, the three interpolation methods produce sharply different orderings of coefficients, with several datasets switching sign or moving from the upper to the lower end of the distribution depending on the interpolation rule. For example, under nearest-neighbour interpolation, CMAP and PERSIANN–CDR produce positive or near-zero coefficients, whereas under bilinear or zonal aggregation they become substantially negative. Conversely, ERA5 and CRU TS move toward the middle of the distribution once spatial smoothing is applied, while CHIRPS and TerraClimate consistently remain among the most negative.

Although the inclusion of controls reduces this volatility, minor rank reversals persist, particularly among coarse-resolution and satellite-only datasets such as CMAP, PERSIANN–CDR, and TAMSAT. These patterns imply that interpolation strategies can meaningfully alter not only the magnitude but also the perceived reliability of rainfall–food insecurity linkages.

Taken together, these findings underscore that rainfall datasets are not affine transformations of one another; they differ systematically in measurement structure, gauge reliance, and spatial precision. Such heterogeneity has direct implications for empirical inference, as it affects which datasets appear more or less sensitive to welfare outcomes and, by extension, which products might be deemed "better performing." Interpolation is therefore not a neutral preprocessing choice; it shapes both statistical inference and substantive interpretation.

Overall, incorporating controls transforms the rainfall–food insecurity relationship from a heterogeneous and sometimes counterintuitive pattern into a coherent and theoretically consistent one. High-resolution and gauge-calibrated products (CHIRPS, TerraClimate, CRU TS) generate the most reliable signals, while satellite-only datasets and coarse reanalyses remain weaker and noisier. Collectively, these results demonstrate that dataset construction and spatial processing choices are central to the credibility and robustness of empirical climate–economy analyses.

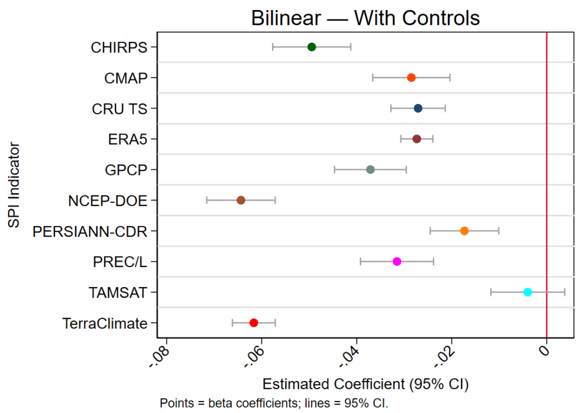

(a) Bilinear interpolation coefficients with controls.

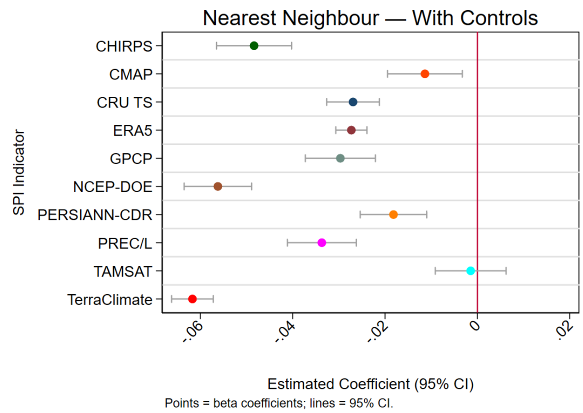

(b) Nearest-neighbor interpolation coefficients with controls.

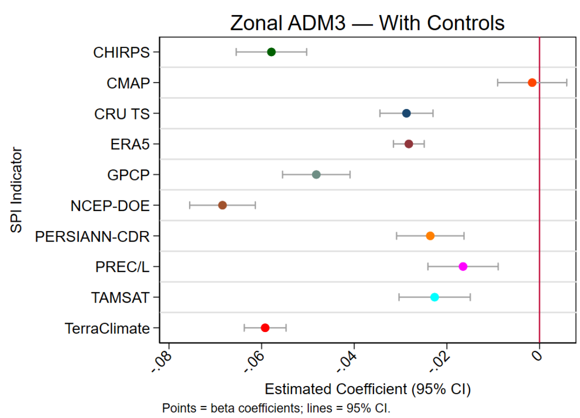

(c) Zonal aggregation coefficients with controls.

Figure 6: Estimated coefficients with household and community controls across interpolation methods.

Note: See Table 1 for the list and summary of the controls.

5 Conclusion

This study demonstrates that estimates of rainfall variability's impact on household food insecurity are highly sensitive to both dataset characteristics and spatial interpolation methods. In models estimated without household- and community-level controls, coefficients vary widely in both sign and magnitude, with several satellite-only products producing positive or near-zero effects. Such heterogeneity reflects the joint influence of omitted-variable bias, measurement error, and differences in dataset resolution, leading to patterns that are inconsistent with theoretical expectations and potentially misleading for policy interpretation.

Once controls are introduced, this instability largely disappears. Across all ten rainfall datasets and the three interpolation techniques, coefficients converge to negative, statistically significant, and broadly consistent values. Zonal aggregation produces the largest-magnitude estimates, reflecting the influence of spatial averaging across administrative regions. Bilinear interpolation yields moderate, stable coefficients, while nearest-neighbour interpolation, previously the most volatile, now produces uniformly negative effects. The dispersion of coefficients across intrapolation methods also narrows sharply. This convergence suggests that the apparent heterogeneity in the uncontrolled estimates primarily arises from unobserved confounders rather than genuine spatial differences in rainfall exposure.

Three methodological insights emerge. First, spatial interpolation is not a neutral preprocessing step. Choices such as aggregation, smoothing, and pixel-level matching materially affect both the magnitude and sign of estimated coefficients. Second, dataset construction, whether satellite-only, gauge-based, or reanalysis, interacts with interpolation method and model specification to produce systematic differences in estimated effects. High-resolution and gauge-calibrated products such as CHIRPS, TerraClimate, and CRU TS consistently generate stable, negative coefficients once controls are applied, whereas satellite-only and coarse-resolution products remain noisier and closer to zero. Third, excluding household- and community-level controls exaggerates or distorts the estimated rainfall effects, increasing the risk of spurious findings and misleading inferences.

From an applied perspective, interpolation strategies should be chosen in line with dataset resolution and research purpose. Nearest-neighbour assignment, especially for coarse-resolution datasets, amplifies measurement error and can produce implausible results, making it unsuitable for micro-level analyses. Bilinear interpolation offers a balanced approach for high-resolution datasets, retaining local variation while limiting volatility. Zonal aggregation, by contrast, is appropriate for policy simulations or studies focused on administrative averages. Gauge-based and reanalysis datasets, once controls are included, perform relatively consistently across interpolation methods, underscoring their robustness for longitudinal or cross-regional analysis.

Finally, these findings underscore the importance of pre-analysis plans in climate–economics research. Explicitly defining datasets, interpolation methods, control variables, and estimation strategies in advance reduces researcher discretion and limits selective reporting. Given the high sensitivity of rainfall–food insecurity estimates to methodological decisions, such safeguards are essential to enhance transparency, reproducibility, and the robustness of empirical conclusions.

References

Abatzoglou, J. T., Dobrowski, S. Z., Parks, S. A., & Hegewisch, K. C. (2018). Terraclimate, a high-resolution global dataset of monthly climate and climatic water balance from 1958–2015. *Scientific data*, 5(1), 1–12.

Abay, K. A. (2020). Measurement errors in agricultural data and their implications on marginal returns to modern agricultural inputs. *Agricultural Economics*, 51(3), 323–341.

Abay, K. A., Abate, G. T., Barrett, C. B., & Bernard, T. (2019). Correlated non-classical mes, 'second best' policy inference, and the inverse size-productivity relationship in agriculture. *Journal of Development Economics*, 139, 171–184.

Abay, K. A., Bevis, L. E., & Barrett, C. B. (2021). Measurement error mechanisms matter: Agricultural intensification with farmer misperceptions and misreporting. *American Journal of Agricultural Economics*, 103(2), 498–522.

Abay, K. A., Wossen, T., Abate, G. T., Stevenson, J. R., Michelson, H., & Barrett, C. B. (2023). Inferential and behavioral implications of measurement error in agricultural data. *Annual Review of Resource Economics*, 15(1), 63–83.

Adler, R. F., Huffman, G. J., Chang, A., Ferraro, R., Xie, P.-P., Janowiak, J., Rudolf, B., Schneider, U., Curtis, S., Bolvin, D., et al. (2003). The version-2 global precipitation climatology project (gpcp) monthly precipitation analysis (1979–present). *Journal of hydrometeorology*, 4(6), 1147–1167.

Alix-Garcia, J., & Millimet, D. L. (2023). Remotely incorrect? accounting for nonclassical measurement error in satellite data on deforestation. *Journal of the Association of Environmental and Resource Economists*, 10(5), 1335–1367.

Amare, M., & Balana, B. (2023). Climate change, income sources, crop mix, and input use decisions: Evidence from nigeria. *Ecological Economics*, 211, 107892.

Amparore, A., Constas, M. A., Fossi, F., Gauny, J., Marsland, N., & Ulimwengu, J. (2023). The data in emergencies (diem) hub for evaluating multiple shock impacts on food security. *Nature Food*, 4(8), 628–629.

Auffhammer, M., Hsiang, S. M., Schlenker, W., & Sobel, A. (2013). Using weather data and climate model output in economic analyses of climate change. *Review of Environmental Economics and Policy*, 7(2), 181–198.

Azzarri, C., & Nico, G. (2022). Sex-disaggregated agricultural extension and weather variability in africa south of the sahara. *World Development*, 155, 105897.

Banerjee, R., & Maharaj, R. (2020). Heat, infant mortality, and adaptation: Evidence from india. *Journal of Development Economics*, 143, 102378.

Bas, M., & Paunov, C. (2025). Riders on the storm: How do firms navigate production and market conditions amid el niño? *Journal of Development Economics*, 172, 103374.

Baysan, C., Dar, M. H., Emerick, K., Li, Z., & Sadoulet, E. (2024). The agricultural wage gap within rural villages. *Journal of Development Economics*, 168, 103270.

Branco, D., & Féres, J. (2021). Weather shocks and labor allocation: Evidence from rural brazil. *American Journal of Agricultural Economics*, 103(4), 1359–1377.

Burke, M., Gong, E., & Jones, K. (2015). Income shocks and hiv in africa. *The Economic Journal*, 125(585), 1157–1189.

Burke, M. B., Miguel, E., Satyanath, S., Dykema, J. A., & Lobell, D. B. (2009). Warming increases the risk of civil war in africa. *Proceedings of the national Academy of sciences*, 106(49), 20670–20674.

Callahan, C. W., & Mankin, J. S. (2022). Globally unequal effect of extreme heat on economic growth. *Science Advances*, 8(43), eadd3726.

Carleton, T. A., & Hsiang, S. M. (2016). Social and economic impacts of climate. *Science*, 353(6304), aad9837.

Chamberlin, J., & Ricker-Gilbert, J. (2016). Participation in rural land rental markets in sub-saharan africa: Who benefits and by how much? evidence from malawi and zambia. *American Journal of Agricultural Economics*, 98(5), 1507–1528.

Chen, M., Xie, P., Janowiak, J. E., & Arkin, P. A. (2002). Global land precipitation: A 50-yr monthly analysis based on gauge observations [Editorial Type: Article; Article Type: Research Article]. *Journal of Hydrometeorology*, 3(3), 249–266. https://doi.org/10.1175/1525-7541(2002)003⟨0249:GLPAYM⟩2.0.CO;2

Colmer, J. (2021). Rainfall variability, child labor, and human capital accumulation in rural ethiopia. *American Journal of Agricultural Economics*, 103(3), 858–877.

Cooper, M. W., Brown, M. E., Hochrainer-Stigler, S., Pflug, G., McCallum, I., Fritz, S., & Zvoleff, A. (2019). Mapping the effects of drought on child stunting. *Proceedings of the National Academy of Sciences*, 116(35), 17219–17224.

Corno, L., Hildebrandt, N., & Voena, A. (2020). Age of marriage, weather shocks, and the direction of marriage payments. *Econometrica*, 88(3), 879–915.

Dasgupta, S., & Robinson, E. J. (2023). Climate, weather and child health in burkina faso. *Australian Journal of Agricultural and Resource Economics*, 67(4), 576–602.

Deschênes, O., & Greenstone, M. (2007). The economic impacts of climate change: Evidence from agricultural output and random fluctuations in weather. *American Economic Review*, 97(1), 354–385.

Di Falco, S., & Han, K. (2025). Mitigating the health impact of a famine: Evidence from the 1985 ethiopian emergency food aid. *Journal of Development Economics*, 103531.

Dillon, A., Gourlay, S., McGee, K., & Oseni, G. (2019). Land measurement bias and its empirical implications: Evidence from a validation exercise. *Economic Development and Cultural Change*, 67(3), 595–624.

Dinkelman, T. (2017). Long-run health repercussions of drought shocks: Evidence from south african homelands. *The Economic Journal*, 127(604), 1906–1939.

Eberhard-Ruiz, A., & Moradi, A. (2019). Regional market integration in east africa: Local but no regional effects? *Journal of Development Economics*, 140, 255–268.

Emediegwu, L. E., Wossink, A., & Hall, A. (2022). The impacts of climate change on agriculture in sub-saharan africa: A spatial panel data approach. *World Development*, 158, 105967.

FAO, IFAD, UNICEF, WFP & WHO. (2024). *The state of food security and nutrition in the world 2024 – financing to end hunger, food insecurity and malnutrition in all its forms* (tech. rep.). Rome.

Feeny, S., Mishra, A., Trinh, T. A., Ye, L., & Zhu, A. (2021). Early-life exposure to rainfall shocks and gender gaps in employment: Findings from vietnam. *Journal of Economic Behavior & Organization*, 183, 533–554.

Felbermayr, G., Gröschl, J., Sanders, M., Schippers, V., & Steinwachs, T. (2022). The economic impact of weather anomalies. *World Development*, 151, 105745.

Fischer, S., Hilger, T., Piepho, H.-P., Jordan, I., & Cadisch, G. (2019). Do we need more drought for better nutrition? the effect of precipitation on nutrient concentration in east african food crops. *Science of the Total Environment*, 658, 405–415.

Fishman, R., Carrillo, P., & Russ, J. (2019). Long-term impacts of exposure to high temperatures on human capital and economic productivity. *Journal of Environmental Economics and Management*, 93, 221–238.

Flores, F. M., Milusheva, S., Reichert, A. R., & Reitmann, A. K. (2024). Climate anomalies and international migration: A disaggregated analysis for west africa. *Journal of Environmental Economics and Management*, 126, 102997.

Fluhrer, S., & Kraehnert, K. (2022). Sitting in the same boat: Subjective well-being and social comparison after an extreme weather event. *Ecological Economics*, 195, 107388.

Fontaine, I., Garabedian, S., & Vérèmes, H. (2024). Tropical cyclones and fertility: New evidence from developing countries. *Ecological Economics*, 226, 108341.

Freudenreich, H., Aladysheva, A., & Brück, T. (2022). Weather shocks across seasons and child health: Evidence from a panel study in the kyrgyz republic. *World Development*, 155, 105801.

Funk, C., Peterson, P., Landsfeld, M., Pedreros, D., Verdin, J., Shukla, S., Husak, G., Rowland, J., Harrison, L., Hoell, A., et al. (2015). The climate hazards infrared precipitation with stations—a new environmental record for monitoring extremes. *Scientific data*, 2(1), 1–21.

Garg, T., Hamilton, S. E., Hochard, J. P., Kresch, E. P., & Talbot, J. (2018). (not so) gently down the stream: River pollution and health in indonesia. *Journal of Environmental Economics and Management*, 92, 35–53.

Gibson, J., Olivia, S., Boe-Gibson, G., & Li, C. M. (2021). Which night lights data should we use in economics, and where? *Journal of Development Economics*, 149, 102602.

Gourlay, S., Kilic, T., & Lobell, D. B. (2019). A new spin on an old debate: Errors in farmer-reported production and their implications for inverse scale-productivity relationship in uganda. *Journal of Development Economics*, 141, 102376.

Gregory, P. J., Ingram, J. S., & Brklacich, M. (2005). Climate change and food security. *Philosophical Transactions of the Royal Society B: Biological Sciences*, 360(1463), 2139–2148.

Gröger, A., & Zylberberg, Y. (2016). Internal labor migration as a shock coping strategy: Evidence from a typhoon. *American Economic Journal: Applied Economics*, 8(2), 123–153.

Gu, Q., Li, S., Tian, S., & Wang, Y. (2024). Impact of climate risk on energy market risk spillover: Evidence from dynamic heterogeneous network analysis. *Energy Economics*, 137, 107775.

Guiteras, R., Jina, A., & Mobarak, A. M. (2015). Satellites, self-reports, and submersion: Exposure to floods in bangladesh. *American Economic Review*, 105(5), 232–236.

Harari, M., & Ferrara, E. L. (2018). Conflict, climate, and cells: A disaggregated analysis. *Review of Economics and Statistics*, 100(4), 594–608.

Harris, I., Osborn, T. J., Jones, P., & Lister, D. (2020). Version 4 of the cru ts monthly high-resolution gridded multivariate climate dataset. *Scientific data*, 7(1), 109.

Harrison, L., Funk, C., & Peterson, P. (2019). Identifying changing precipitation extremes in sub-saharan africa with gauge and satellite products. *Environmental Research Letters*, 14(8), 085007.

Hazrana, J., Birthal, P. S., & Mishra, A. K. (2025). Equal exposure, unequal effects of climate change: Gendered impacts on food consumption and nutrition in rural bangladesh. *Ecological Economics*, 230, 108486.

Hersbach, H., Bell, B., Berrisford, P., Hirahara, S., Horányi, A., Muñoz-Sabater, J., Nicolas, J., Peubey, C., Radu, R., Schepers, D., et al. (2020). The era5 global reanalysis. *Quarterly journal of the royal meteorological society*, 146(730), 1999–2049.

Hotte, R., & Lambert, S. (2023). Marriage payments and wives' welfare: All you need is love. *Journal of Development Economics*, 164, 103141.

Hsiang, S. M., Meng, K. C., & Cane, M. A. (2011). Civil conflicts are associated with the global climate. *Nature*, 476(7361), 438–441.

Huang, J., Yu, H., Guan, X., Wang, G., & Guo, R. (2016). Accelerated dryland expansion under climate change. *Nature climate change*, 6(2), 166–171.

Huffman, G. J., Adler, R. F., Bolvin, D. T., Gu, G., Nelkin, E. J., Bowman, K. P., Hong, Y., Stocker, E. F., & Wolff, D. B. (2001). Global precipitation at one-degree daily resolution from multisatellite observations. *Journal of Hydrometeorology*, 2(1), 36–50.

Jagnani, M., Barrett, C. B., Liu, Y., & You, L. (2021). Within-season producer response to warmer temperatures: Defensive investments by kenyan farmers. *The Economic Journal*, 131(633), 392–419.

Jain, M. (2020). The benefits and pitfalls of using satellite data for causal inference. *Review of Environmental Economics and Policy*.

Jayachandran, S. (2006). Selling labor low: Wage responses to productivity shocks in developing countries. *Journal of Political Economy*, 114(3), 538–575.

Jolly, W. M., Cochrane, M. A., Freeborn, P. H., Holden, Z. A., Brown, T. J., Williamson, G. J., & Bowman, D. M. (2015). Climate-induced variations in global wildfire danger from 1979 to 2013. *Nature communications*, 6(1), 7537.

Josephson, A., Michler, J. D., Kilic, T., & Murray, S. (2026). The mismeasure of weather: Using earth observation data for estimation of socioeconomic outcomes. *Journal of Development Economics*, 178, 103553.

Kalkuhl, M., & Wenz, L. (2020). The impact of climate conditions on economic production. evidence from a global panel of regions. *Journal of Environmental Economics and Management*, 103, 102360.

Kanamitsu, M., Ebisuzaki, W., Woollen, J., Yang, S.-K., Hnilo, J. J., Fiorino, M., & Potter, G. L. (2002). Ncep–doe amip-ii reanalysis (r-2). *Bulletin of the American Meteorological Society*, 83(11), 1631–1643. https://doi.org/10.1175/BAMS-83-11-1631

Kang, H., Sridhar, V., Mainuddin, M., & Trung, L. D. (2021). Future rice farming threatened by drought in the lower mekong basin. *Scientific reports*, 11(1), 9383.

Kosmowski, F., Chamberlin, J., Ayalew, H., Sida, T., Abay, K., & Craufurd, P. (2021). How accurate are yield estimates from crop cuts? evidence from smallholder maize farms in ethiopia. *Food Policy*, 102, 102122.

Leroux, L., Castets, M., Baron, C., Escorihuela, M. J., Bégué, A., & Seen, D. L. (2019). Maize yield estimation in west africa from crop process-induced combinations of multi-domain remote sensing indices. *European Journal of Agronomy*, 108, 11–26.

Maccini, S., & Yang, D. (2009). Under the weather: Health, schooling, and economic consequences of early-life rainfall. *American Economic Review*, 99(3), 1006–1026.

Maidment, R. I., Grimes, D., Allan, R. P., Tarnavsky, E., Stringer, M., Hewison, T., Roebeling, R., & Black, E. (2014). The 30 year tamsat african rainfall climatology and time series (tarcat) data set. *Journal of Geophysical Research: Atmospheres*, 119(18), 10–619.

Mason-D'Croz, D., Sulser, T. B., Wiebe, K., Rosegrant, M. W., Lowder, S. K., Nin-Pratt, A., et al. (2019). Agricultural investments and hunger in africa modeling potential contributions to sdg2–zero hunger. *World development*, 116, 38–53.

McKee, T. B., Doesken, N. J., & Kleist, J. (1993). The relationship of drought frequency and duration to time scales. *Proceedings of the 8th Conference on Applied Climatology*, 179–184.

Meyer, B. D., & Mittag, N. (2017). Misclassification in binary choice models. *Journal of Econometrics*, 200(2), 295–311.

Michler, J. D., Baylis, K., Arends-Kuenning, M., & Mazvimavi, K. (2019). Conservation agriculture and climate resilience. *Journal of environmental economics and management*, 93, 148–169.

Michler, J. D., Josephson, A., Kilic, T., & Murray, S. (2022). Privacy protection, measurement error, and the integration of remote sensing and socioeconomic survey data. *Journal of Development Economics*, 158, 102927.

Miguel, J. D. N. (2024). Returns to quality in rural agricultural markets: Evidence from wheat markets in ethiopia. *Journal of Development Economics*, 171, 103336.

Minor, K., Bjerre-Nielsen, A., Jonasdottir, S. S., Lehmann, S., & Obradovich, N. (2022). Rising temperatures erode human sleep globally. *One Earth*, 5(5), 534–549.

Mueller, B., & Seneviratne, S. I. (2012). Hot days induced by precipitation deficits at the global scale. *Proceedings of the national academy of sciences*, 109(31), 12398–12403.

Nguyen, P., Ombadi, M., Gorooh, V. A., Shearer, E. J., Sadeghi, M., Sorooshian, S., Hsu, K., Bolvin, D., & Ralph, M. F. (2020). Persiann dynamic infrared–rain rate (pdir-now): A near-real-time, quasi-global satellite precipitation dataset. *Journal of hydrometeorology*, 21(12), 2893–2906.

Obradovich, N., Migliorini, R., Mednick, S. C., & Fowler, J. H. (2017). Nighttime temperature and human sleep loss in a changing climate. *Science advances*, 3(5), e1601555.

Omiat, G., & Shively, G. (2020). Rainfall and child weight in uganda. *Economics & Human Biology*, 38, 100877.

Physical Sciences Laboratory. (n.d.). Noaa's gridded precipitation reconstruction (prec) [Accessed: 2025-08-14]. *NOAA Physical Sciences Laboratory*.

Ricker-Gilbert, J., & Jones, M. (2015). Does storage technology affect adoption of improved maize varieties in africa? insights from malawi's input subsidy program. *Food policy*, 50, 92–105.

Rocha, R., & Soares, R. R. (2015). Water scarcity and birth outcomes in the brazilian semiarid. *Journal of Development Economics*, 112, 72–91.

Rosales-Rueda, M. (2018). The impact of early life shocks on human capital formation: Evidence from el niño floods in ecuador. *Journal of Health Economics*, 62, 13–44.

Russo, S., Sillmann, J., & Sterl, A. (2017). Humid heat waves at different warming levels. *Scientific reports*, 7(1), 7477.

Sakketa, T. G., Maggio, D., & McPeak, J. (2025). The protective role of index insurance in the experience of violent conflict: Evidence from ethiopia. *Journal of Development Economics*, 174, 103445.

Schwalm, C. R., Anderegg, W. R., Michalak, A. M., Fisher, J. B., Biondi, F., Koch, G., Litvak, M., Ogle, K., Shaw, J. D., Wolf, A., et al. (2017). Global patterns of drought recovery. *Nature*, 548(7666), 202–205.

Sedova, B., & Kalkuhl, M. (2020). Who are the climate migrants and where do they go? evidence from rural india. *World Development*, 129, 104848.

Sekhri, S., & Storeygard, A. (2014). Dowry deaths: Response to weather variability in india. *Journal of development economics*, 111, 212–223.

Sheffield, J., Goteti, G., & Wood, E. F. (2006). Development of a 50-year high-resolution global dataset of meteorological forcings for land surface modeling. *Journal of climate*, 19(13), 3088–3111.

Smith, C., Baker, J., & Spracklen, D. (2023). Tropical deforestation causes large reductions in observed precipitation. *Nature*, 615(7951), 270–275.

Sorooshian, S., Hsu, K.-L., Gao, X., Gupta, H. V., Imam, B., & Braithwaite, D. (2000). Evaluation of the persiann system satellite-based estimates of tropical rainfall. *Bulletin of the American Meteorological Society*, 81(9), 2035–2046. https://doi.org/10.1175/1520-0477(2000)081⟨2035:EOPSSE⟩2.3.CO;2

Tzachor, A., Richards, C. E., Gudoshava, M., Nying'uro, P., Misiani, H., Ongoma, J. G., et al. (2023). How to reduce africa's undue exposure to climate risks. *Nature*, 620(7974), 488–491.

Ubilava, D., Hastings, J. V., & Atalay, K. (2023). Agricultural windfalls and the seasonality of political violence in africa. *American Journal of Agricultural Economics*, 105(5), 1309–1332.

Van der Merwe, E., Clance, M., & Yitbarek, E. (2022). Climate change and child malnutrition: A nigerian perspective. *Food Policy*, 113, 102281.

Wagner, J., Koehler, J., Dupuis, M., & Hope, R. (2024). Is volumetric pricing for drinking water an effective revenue strategy in rural mali? *npj Clean Water*, 7(1), 57.

World Bank. (2022, May). Mali economic update: Resilience in uncertain times – renewing the social contract [Accessed: 2025-07-07].

World Bank. (2023). The world bank group in chad, fiscal years 2010–20: Country program evaluation [Accessed: 2025-07-07].

World Bank. (2025a). Chad overview [Accessed: 2025-07-07].

World Bank. (2025b). The world bank in mali [Accessed: 2025-07-07].

Wossen, T., Abdoulaye, T., Alene, A., Nguimkeu, P., Feleke, S., Rabbi, I. Y., et al. (2019). Estimating the productivity impacts of technology adoption in the presence of misclassification. *American Journal of Agricultural Economics*, 101(1), 1–16.

Zhang, B., Wang, S., Zscheischler, J., & Moradkhani, H. (2023). Higher exposure of poorer people to emerging weather whiplash in a warmer world. *Geophysical Research Letters*, 50(21), e2023GL105640.

Appendices

A Appendix

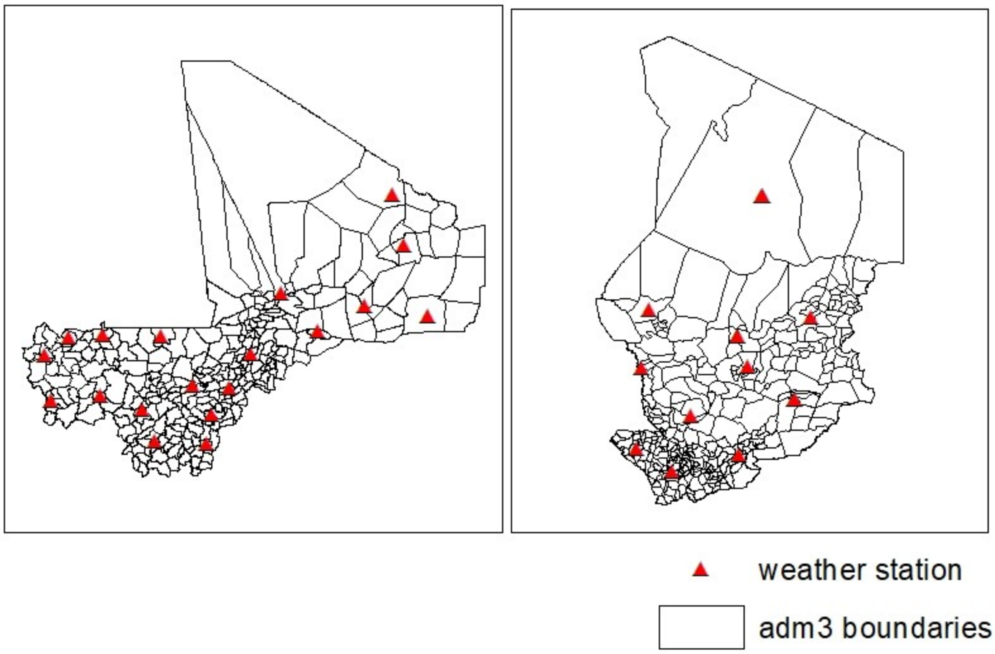

Figure A1: In-Country Weather Stations

Note: The figure shows the distribution of weather stations in Mali (left) and Chad (right). *Source:* Most recent data retrieved from NOAA's GHCN dataset.

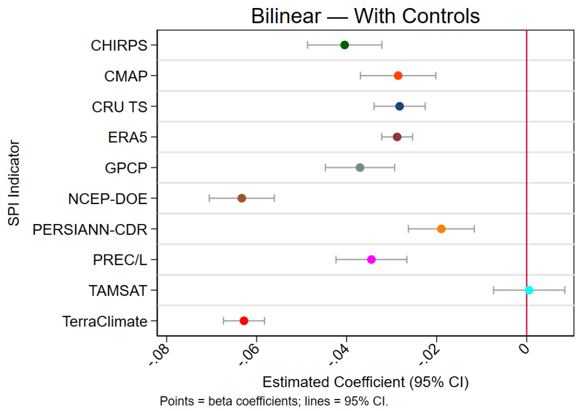

(a) Bilinear interpolation coefficients with controls.

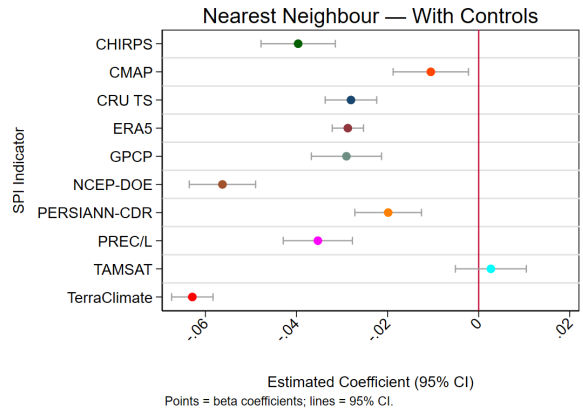

(b) Nearest-neighbor interpolation coefficients with controls.

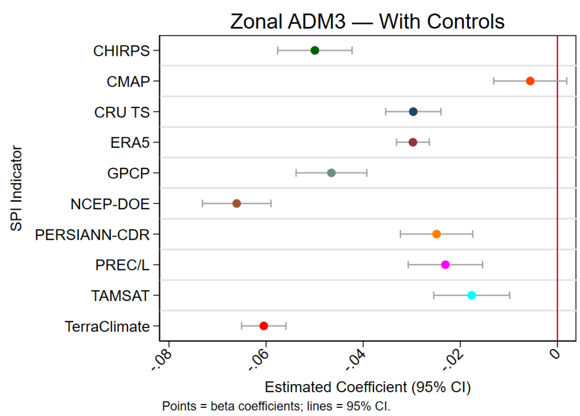

(c) Zonal aggregation coefficients with controls.

Figure A2: Estimated coefficients with household and community controls across interpolation methods.

Note: See Table 1 for the list and summary of the controls.

B Appendix

Table B1: Pearson correlation coefficients (r) between reported drought shock and SPI (Gamma-based) from ten precipitation datasets.

Dataset	Bilinear interpolation	Nearest neighbor	Zonal averaging
CHIRPS	-0.1776***	-0.1733***	-0.1657***
CMAP	-0.2050***	-0.2039***	-0.1772***
CRU TS	-0.1483***	-0.1500***	-0.1537***
ERA5	-0.1563***	-0.1563***	-0.1592***
GPCP	-0.0947***	-0.1027***	-0.0876***
NCEP-DOE	-0.0237***	-0.0228***	-0.0234***
PERSIANN-CDR	-0.0906***	-0.0919***	-0.0997***
PREC/L	-0.1824***	-0.1803***	-0.1360***
TAMSAT	-0.1159***	-0.1122***	-0.1160***
TerraClimate	-0.2000***	-0.1997***	-0.2050***

Note: Values represent Pearson correlation coefficients (r) between self-reported drought shock experience and SPI derived from precipitation estimates fitted to a Gamma distribution. Significance levels: $^{***}p < 0.01$, $^{**}p < 0.05$, $^{*}p < 0.1$.

Table B2: Pearson correlation coefficients (r) between total income and SPI from ten precipitation datasets.

Dataset	Bilinear interpolation	Nearest neighbor	Zonal averaging
CHIRPS	0.0503***	0.0553***	0.0635***
CMAP	0.0498***	0.0278***	-0.0643***
CRU TS	0.1494***	0.1515***	0.1504***
ERA5	0.0545***	0.0541***	0.0552***
GPCP	0.0931***	0.0806***	0.0885***
NCEP-DOE	0.1290***	0.1299***	0.1174***
PERSIANN-CDR	-0.0028	-0.0025	-0.0042
PREC/L	0.0560***	0.0456***	-0.0513***
TAMSAT	0.0230***	0.0227***	0.0381***
TerraClimate	0.1062***	0.1062***	0.0977***

Note: Values represent Pearson correlation coefficients (r) between total household income and Standardized Precipitation Index (SPI). Significance levels: $^{***}p < 0.01$, $^{**}p < 0.05$, $^{*}p < 0.1$.

Table B3: Summary statistics of FIES items (30-day recall)

FIES item	Mean	Std. Dev.
Worried about not having enough food to eat	0.808	0.394
Unable to eat healthy and nutritious food	0.675	0.468
Ate only a few kinds of foods	0.697	0.460
Had to skip a meal	0.592	0.491
Ate less than you thought you should	0.609	0.488
Ran out of food	0.295	0.456
Were hungry but did not eat	0.360	0.480
Went without eating for a whole day	0.128	0.334

Note: The first eight items are the standardized FIES questions. Respondents were asked: 'During the last 30 days, was there a time when you or others in your household experienced the following due to lack of money or other resources?' Each item is coded as a binary indicator (1 = yes, 0 = no).